Hindawi
Journal of Nanomaterials
Volume 2018, Article ID 1506342, 7 pages
https://doi.org/10.1155/2018/1506342

Research Article

A Magnetic and pH-Sensitive Composite Nanoparticle for Drug Delivery

Xin Wang, Ziyu Gao, Long Zhang, Huiming Wang, and Xiaohong Hu

School of Material Engineering, Jinling Institute of Technology, Nanjing 211169, China

Correspondence should be addressed to Xiaohong Hu; hxh@jit.edu.cn

Received 21 November 2017; Revised 6 April 2018; Accepted 12 April 2018; Published 20 May 2018

Academic Editor: Andrew R. Barron

Mild acid response nanocarriers have been intensively attracted interest in the field of drug delivery on the account of the responsive property to abnormal physiological environment as well as the original property to normal physiological environment. However, the drug delivery system lacks capacity of precise localization to abnormal tissue or targeted cells. Therefore, a magnetic and pH-sensitive composite nanoparticle was designed and prepared by double water-in-oil-in-water (W/O/W) emulsion using acetylated β-cyclodextrin (Ac-β-CD) as a dominant material to realize the pH response and Fe_3O_4 as a component to realize magnetic response. The surface chemical characteristic was characterized by Fourier-transformed infrared spectroscopy (FTIR) using pure Ac-β-CD nanoparticle as a control and exhibits the typical chemical characteristic of Ac-β-CD. Furthermore, the structural information was tracked by X-ray diffraction (XRD) and thermogravimetric analysis (TG). It was found that composite nanoparticle possessed structural characteristic of both Ac-β-CD and Fe_3O_4. Composite nanoparticle exhibited sphere and two-phase morphology with the diameter of about 200–250 nm depending on their detection method and zeta potential of −12 to −14 mV. More importantly, irreversible pH response property and reversible magnetic responsive properties either in neutral environment or in mild acid environment for the composite nanoparticle were confirmed in the research. Finally, drug loading and release behavior were investigated through preliminary in vitro evaluation.

1. Introduction

Stimulus-response nanoparticles attract increasing interest on the account of adjustable property response to stimulus of externalities [1–10]. Among these, acid response nanoparticle and magnetic response nanoparticle are frequently used as drug carriers in view of the difference between normal physiological environment (pH 7.4) and abnormal physiological environment (pH lower than 6.0) [4–8, 10]. Further, since biocompatibility and biodegradability are fundamental requests for a drug carrier, a large number of natural polymers like peptides, proteins, and polysaccharides have been chosen to fabricate nanocarriers for drug delivery due to their good biocompatibility and natural biodegradability [10–13]. However, in most cases, traditional natural polymers lacked of a responsive functional group that response to external stimulus, which restricted their application. Recently, the emerging of acetylated polysaccharides, which had response to acid environment (pH 5.5–6.0) due to the dissolution of acetylated groups, changed the situation [7, 14, 15]. Thus, in the recent research including our own research, the acetylated materials have been intensively concerned and prepared to various carriers including nanoparticle, composite nanocarrier, and nanofiber for drug delivery, gene delivery, and RNA delivery [7, 14, 15]. Although these acid-responsive nanocarriers had succeeded to realize the effective delivery of drug to intracell or abnormal tissue, they were hardly delivered to targeted cell or tissue on the account of lacking the antibody recognition system or targeting system. Therefore, dual-response nanoparticle is still needed for more effective drug or gene delivery.

Targeting drug delivery system is proven to be effective methods for precise location [16, 17]. Magnetic response property was another frequently used method to design and prepare a passive targeting nanocarrier system, which can aggregate objective tissue under the action of the magnetic field. Generally, magnetic nanoparticle is Fe_3O_4 prepared by a hydrothermal method [5, 6]. But pure Fe_3O_4 nanoparticle

is easy to aggregate and lacks biocompatibility. Thus, surface modification using functional polymers was often used to enhance their biocompatibility and improve their dispersibility [15]. In view of their good biocompatibility and natural biodegradability, natural amphiphilic compounds were ideal modifiers for the surface modification of Fe_3O_4 nanoparticle. Therefore, in the work, a magnetic and pH-sensitive composite nanoparticle was designed using Fe_3O_4 nanoparticle as cores endowing magnetic property and acetylated material as a continuous phase of nanocarrier endowing pH response property. Simultaneously, acetylated material could play a role in stabilizing Fe_3O_4 nanoparticle.

In the field of drug delivery, β-cyclodextrin (β-CD) has been intensively used because inclusion effects between β-CD molecules and drug molecules could help drug loading and control drug releasing [15, 18, 19]. Based on these foundations, biocompatible acetylated β-CD (Ac-β-CD) nanoparticle was previously synthesized and fabricated by a single microemulsion evaporation method using gelatin as an emulsifier, which endowed the biocompatibility to nanoparticle. Then, various pH-responsive cyclodextrin-based nanoparticle composite hydrogels were prepared for drug delivery. Since the microemulsion method was an effective and efficient method to fabricate Ac-β-CD nanoparticle, double emulsion was applied to prepare Fe_3O_4 composite Ac-β-CD nanoparticle in consideration of water dispersibility for Fe_3O_4 nanoparticle in the work.

2. Experiment Section

2.1. Materials. Gelatin, β-cyclodextrin (β-CD), 2-methoxypropene, pyridinium 4-toluenesulfonate, anhydrous dimethyl sulfoxide (DMSO), and dichloromethane (DCM) were purchased from Shanghai Medicine and Chemical Company, China. Camptothecin (CPT) and dialysis tube (Mw: 8000–14,000) were from Sigma. Fe_3O_4 nanoparticle (20 nm) was bought from Nanjing Emperor Nano Material Co. Ltd. All other reagents and solvents were of analytical grade and used as received.

2.2. Synthesis of Magnetic and pH-Sensitive Composite Nanoparticle. In the first step, acetylated β-CD (Ac-β-CD) was synthesized according to acetylation reaction [15]. Briefly, 20 times of 2-methoxypropene was reacted with β-CD in anhydrous DMSO for 1 h at 30°C and catalyzed by 5 mM pyridinium *p*-toluene sulfonate. Ac-β-CD was obtained by precipitation in basic water, filtration, and lyophilization.

Magnetic and pH-sensitive composite nanoparticles were prepared by a double microemulsion method. Briefly, Fe_3O_4 nanoparticle was dispersed in 3% gelatin solution (pH 7.5) to obtain 1 mg/mL or 0.1 mg/mL Fe_3O_4 nanoparticle solution, which was emulsified via probe sonication (Scientz, JY92-II) into 1 mL of 10% *w*/*v* Ac-β-CD/DCM solution. The obtained emulsion was further emulsified into 6 mL of 3% *w*/*v* gelatin solution, which was immediately added into 20 mL of 1% *w*/*v* gelatin solution to evaporate DCM under stirring. After 10 h, composite nanoparticles were collected by centrifugation (14,000 rpm, 10 min), washed by basic water, and lyophilized in the end. Composite nanoparticle from 1 mg/mL Fe_3O_4 nanoparticle was denoted as com-nano 1; composite nanoparticle from 0.1 mg/mL Fe_3O_4 nanoparticle was denoted as com-nano 2.

2.3. Characterization of Nanoparticles. The final composite nanoparticles were characterized by Fourier-transformed infrared spectroscopy (FTIR, Nicolet IS10) using pure Ac-β-CD nanoparticle and the previous method as a control. The structural information was characterized by X-ray diffraction (XRD, Advance D8) using pure Fe_3O_4 nanoparticle as a control, thermogravimetric analysis (TG, STA409), dynamic light scattering (DLS, nano ZS), transmission electron microscope (TEM, Tecnai 12), and vibrating sample magnetometer (VSM, Squid-VSM). The magnetic and pH response property was tracked by observation and confirmed by optical photos.

2.4. In Vitro Evaluation of Drug Loading and Releasing Behavior. An anticancer drug (CPT) was chosen as a model drug to be encapsulated into abovementioned nanoparticle during the process of nanoparticle fabrication. Briefly, 1 mg/mL Fe_3O_4 nanoparticle solution was emulsified via probe sonication (Scientz, JY92-II) into 1 mL of 10% *w*/*v* Ac-β-CD/DCM solution containing 5 mg/mL CPT using 100 μL DMSO as a cosolvent for CPT, which was further emulsified via probe sonication into 3% gelatin aqueous solution, just as mentioned above. Final drug loading nanoparticles were obtained by centrifugation (14,000 rpm, 10 min), washed by basic water, and lyophilized, just as mentioned above.

Quantification of CPT was accomplished by a spectrophotometric method. Firstly, nanoparticle suspension was dialyzed in 15 mL 1 mM HCL solution to dissolve all nanoparticles to qualify the loading CPT amount. Absorbance of HCL dialysis solution at 360 nm was detected by UV spectroscopy (Cary 50). The loading CPT amount was obtained by calculation of the absorbance by referring to the standard curve. Secondly, for CPT release assay, nanoparticle suspension was dialyzed in 15 mL water solution with different pH values. At appropriate intervals, 3 mL released dialysis solution was withdrawn and recorded the absorbance at 360 nm to calculate the cumulative CPT release amount using the same method. Simultaneously, 3 mL fresh solution was supplemented into dialysis solution.

3. Result and Discussion

The magnetic and pH-sensitive composite nanoparticle was obtained by a double emulsion method, which was shown in Figure 1. In the procedure, Fe_3O_4 nanoparticle was incorporated and encapsulated in Ac-β-CD solution by emulsification, which formed W/O first emulsion. Then, composite nanoparticle was formed after solvent of DCM was evaporated in W/O/W second emulsion. Herein, 3 kinds of nanoparticle had been fabricated using the condition in Table 1.

In order to clarify the surface characteristic, composite nanoparticle was detected by FTIR using pure Ac-β-CD as a control, as shown in Figure 2. According to the previous

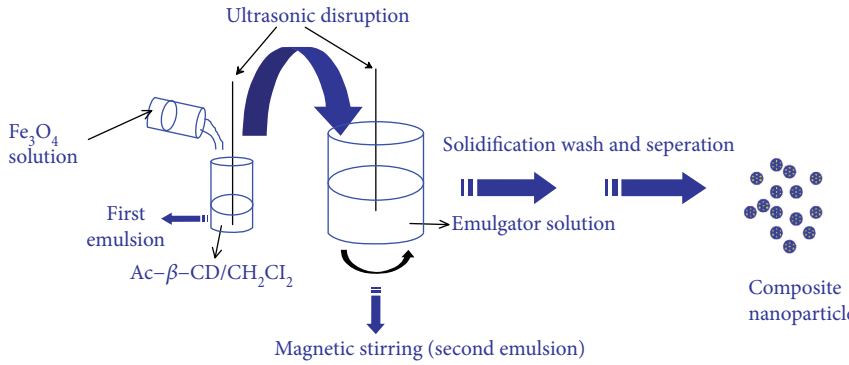

Figure 1: Schematic illustration to show the formation of magnetic and pH-sensitive composite nanoparticle.

Table 1: The fabrication condition and characterizations of composite nanoparticles.

Entry	Preparative parameters	Characterization			
	Weight ratio of Fe_3O_4 and Ac-β-CD	Diameter (nm)	Hydrodynamic diameter Eff. diam. (nm)	PDI	Zeta potential (mV)
Ac-β-CD nano	0 : 10	194 ± 60	253	0.150	−12.1 ± 7.3
Com-nano 1	1 : 10	183 ± 38	234	0.164	−13.8 ± 8.4
Com-nano 2	10 : 10	206 ± 74	224	0.203	−12.7 ± 4.2

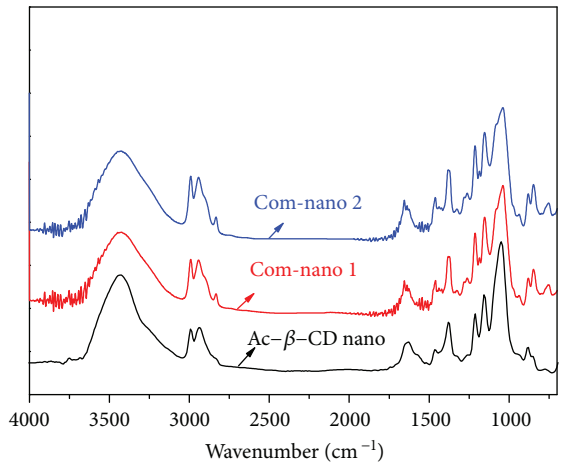

Figure 2: FTIR spectra of Ac-β-CD nanoparticle and magnetic composite Ac-β-CD nanoparticles.

research, the absorbance bands at 2991, 2937, and 1377 cm^{-1} that are characteristic bands for the -$C(CH_3)_2$ group, as well as the significant attenuated absorption at 3427 cm^{-1} due to hydroxyl group, suggested the structure of acetal groups. Moreover, absorbance bands at 1446 cm^{-1} belonging to carboxylic acid peak suggested the existence of gelatin. No obvious difference was found among the three samples, which indicated that they had similar chemical structure on the surface of nanoparticle. These results indicated that composite nanoparticle exhibited similar surface chemical characteristic to pure Ac-β-CD nanoparticle. That was, the composite nanoparticle possessed similar properties to pure Ac-β-CD nanoparticle, especially for those properties related to surface characteristic. For example, since pH-sensitive property was due to degradation of acetal groups on the surface of nanoparticle, composite nanoparticle possessed similar pH-responsive property. In another aspect, Fe_3O_4 did not appear in the surface of composite nanoparticle.

The structural information was characterized by XRD (Figure 3) using pure Fe_3O_4 as a control. The diffraction patterns for Fe_3O_4 have mainly six sharp peaks at 30.4°, 35.6°, 43.3°, 53.2°, 56.9°, and 62.7°, corresponding to (2 2 0), (3 1 1), (4 0 0), (4 2 2), (5 1 1), and (4 4 0) of crystal structure (JCPDS number 001-1111). But differently, for composite nanoparticle, broad peaks at 17.7°, 30.7°, and 41.1° belonging to amorphous state of Ac-β-CD were obviously found in Figure 3. Not surprisingly, the structure of Ac-β-CD played a dominant role in the XRD spectrum since Ac-β-CD was predominantly located in composite nanoparticle (Table 1). Besides these, for com-nano 1, small sharp peaks at 35.6°, 56.9°, and 62.7° were also located in the XRD spectrum, which confirmed the existence of small amount of Fe_3O_4 structures; for com-nano 2, small sharp peaks were hardly witnessed in the XRD spectrum, which was due to a higher weight ratio of Ac-β-CD to Fe_3O_4. Combined with the abovementioned FTIR result, Fe_3O_4 was assumed to encapsulate in the interior of composite nanoparticle.

Two-stage weight loss was witnessed for composite nanoparticle in the TG curve from room temperature to 600°C in Figure 4. In view of composite nanoparticle, unstable groups such as bound water and acetal groups were first degraded under the high temperature environment, then covalent bond between carbons of β-CD could be degraded at several hundred degrees centigrade, but Fe_3O_4 was stable at that temperature. Therefore, the obvious 20% weight loss between 200°C and 230°C was due to the loss of bound water as well as degradation of acetal groups, and the obvious 60% weight

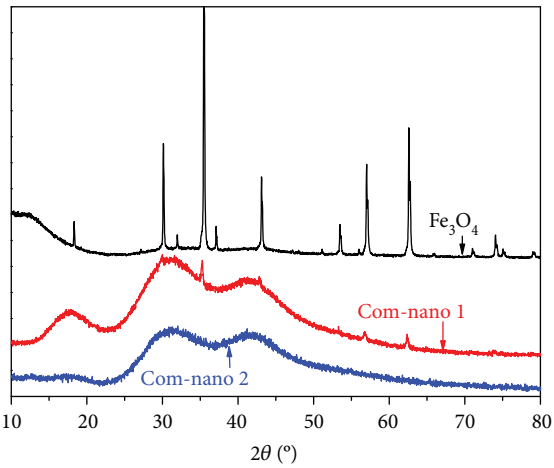

Figure 3: XRD spectra of Fe_3O_4 and magnetic composite Ac-β-CD nanoparticles.

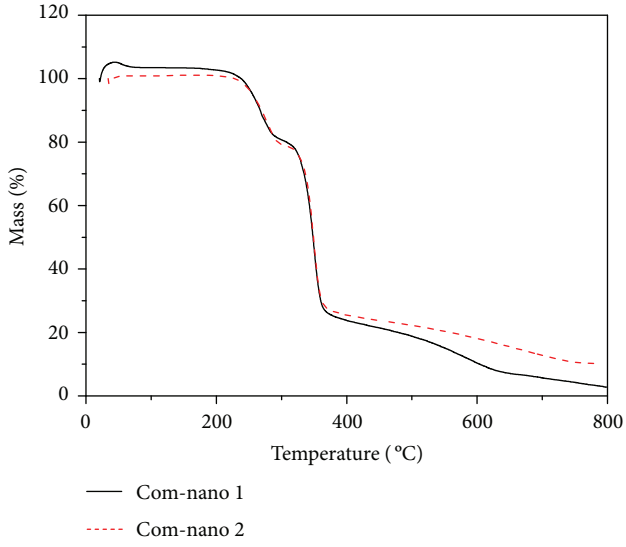

Figure 4: TG curve of magnetic composite Ac-β-CD nanoparticles.

loss at 330°C was due to the whole degradation of β-CD. For com-nano 1, 10% slow weight loss between 350°C and 600°C was witnessed, which was due to the slow degradation of Fe_3O_4 nanoparticle, but for com-nano 2, no another slow weight loss between 350°C and 600°C was found due to less Fe_3O_4 amount in nanoparticle.

The information of nanoparticle's size and morphology was detailed and listed in Table 1 and shown in Figure 5. Composite nanoparticle exhibited sphere morphology and obvious two-phase structure with the continuous phase and multicore phase (Figure 5). Additionally, the continuous phase was assumed to be Ac-β-CD since it is a dominant material for composite nanoparticle; inner cores were assumed to be Fe_3O_4 nanoparticle with suitable size. Average diameter size of composite nanoparticle was about 200 nm (Table 1), regardless of Fe_3O_4 nanoparticle concentration. The effective diameter of nanoparticles by DLS detection was between 220 nm and 250 nm, and no significant difference was found among different nanoparticles in view of Fe_3O_4 nanoparticle concentration, which was consisted with TEM results. Differently, the diameter by the DLS test was larger than that by TEM images, which might be a reason of a larger hydrated radius in solution than died radius. Moreover, the zeta potential is between −12 mV and −14 mV without obvious significant difference among nanoparticles. The results further confirmed the inner and outer structures of composite nanoparticle.

The pH-responsive property of Ac-β-CD nanoparticle, which was induced by degradation of acetal groups and witnessed by transparency variation of nanoparticle solution, had been confirmed by the previous research [15]. Along transparency difference, surface morphology was also witnessed its pH-responsive property [15]. Moreover, pH-sensitive range and responsive time of Ac-β-CD could be adjusted according to the structure of Ac-β-CD. The detailed description was listed in our previous research [15]. Just as above-mentioned, composite nanoparticle possessed similar pH-responsive property to Ac-β-CD nanoparticle. Therefore, no systematic investigation of pH-responsive property was needed for composite nanoparticle; just a simple proven method of observation for transparency of nanoparticle solution was used in the research, which was shown in Figure 6. Simultaneously, magnetic responsive properties of com-nano 1 were also shown in Figure 6. In neutral solution, com-nano 1 could disperse homogeneously with white-black color. Under magnetization, nanoparticles were reversibly attracted to the side of magnetic field leaving half-transparent solution, which confirmed the magnetic responsive properties of com-nano 1. After the magnetic field was removed, the solution could recover the original homogeneously white-black color. Furthermore, if the pH value of solution is adjusted to 5.5, the solution became transparent with black color, which indicated the degradation of acetal groups and the dissolution of Ac-β-CD according to the previous research. But differently, the process is irreversible. In addition, dissolved nanoparticle exhibited reversible magnetic responsive properties in acid solution (pH 5.5). All these results confirmed that com-nano 1 had pH-responsive and magnetic responsive properties. Unfortunately, com-nano 2 had not exhibited obvious pH-responsive and magnetic responsive properties.

In order to characterize the magnetic property, magnetic hysteresis curves of com-nano 1 and acid dissolved com-nano 1 were measured at room temperature over the range of −8 to 8 kOe in Figure 7(b) using Fe_3O_4 nanoparticle as a control (Figure 7(a)). The saturation magnetization of com-nano 1 and acid dissolved com-nano 1 was calculated to be 0.2 and 0.8 emu/g, respectively. Although the saturation magnetization of either com-nano 1 or acid dissolved com-nano 1 was very low compared with the saturation magnetization of Fe_3O_4 nanoparticle, nanoparticle still possessed operable responsive property. Composite nanoparticles exhibited obvious two-phase structure with the continuous phase and multicore phase.

Finally, in vitro evaluation of drug loading and releasing using CPT as a model drug was conducted to investigate the potency nanoparticle as drug carriers. Based on the fact

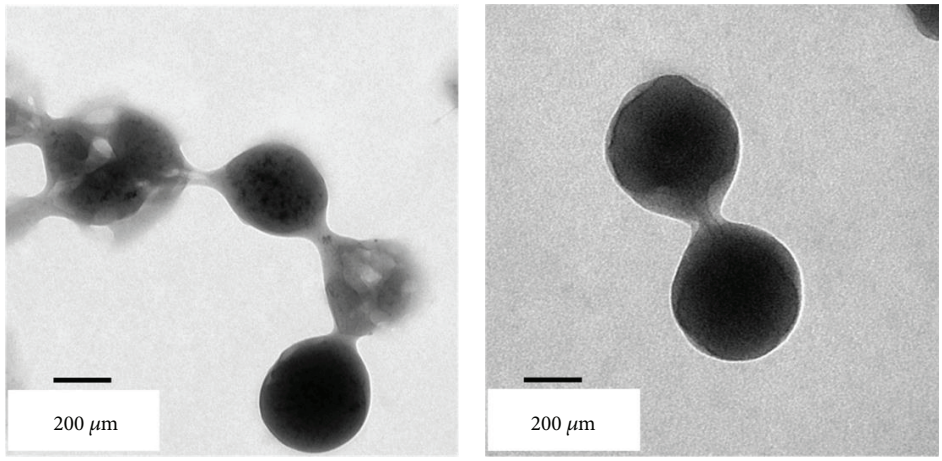

Figure 5: TEM images of (a) com-nano 1 and (b) com-nano 2.

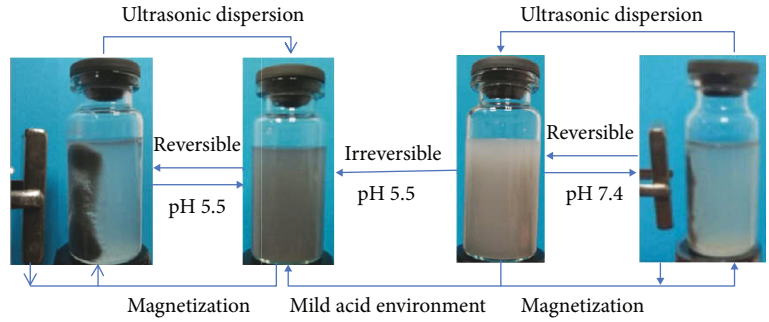

Figure 6: The pH-responsive and magnetic properties of com-nano 1.

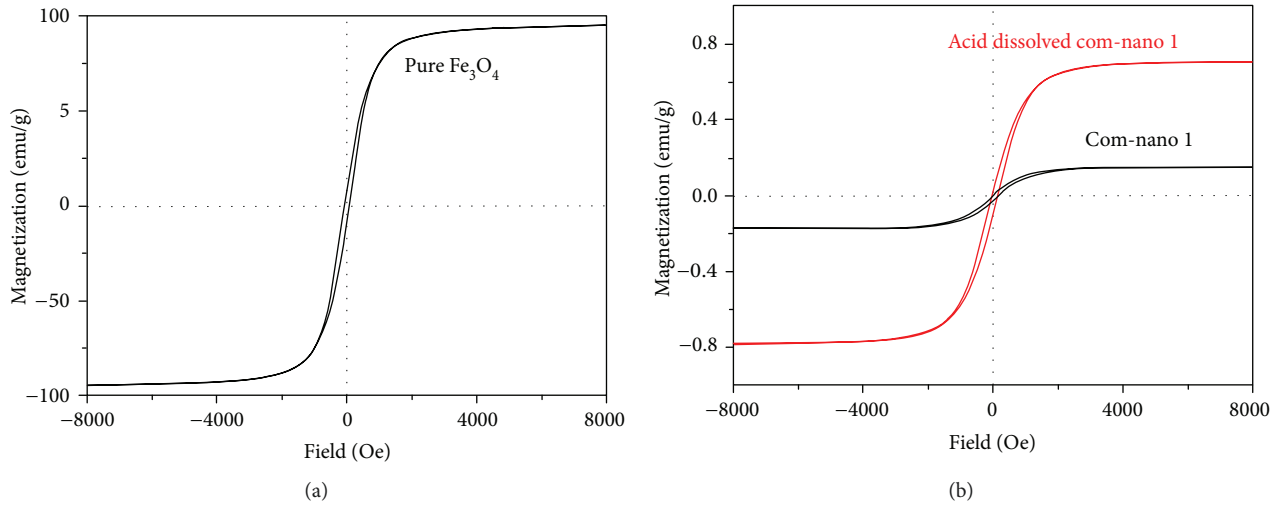

Figure 7: Magnetic hysteresis curves of Fe_3O_4 (a) and com-nano 1 and acid dissolved com-nano 1 (b) at room temperature.

that CPT was encapsulated in nanoparticle as a form of solution and unencapsulated CPT was removed from the nanoparticle system, it was found that drug loading efficiency was 75%. The solubility in pH 7.4 is investigated by the previous research [20]. Moreover, the CPT solubility in medium pH 5.5 was about 7.25 μg/mL, which had no significant difference with its correspondent solubility in medium pH 7.4. Therefore, we think that the drug release behavior shown in Figure 8 is real pH-sensitive release, not apparent. In neutral environment (pH 7.4), drug could be gradually released from com-nano 1 in the beginning 20 h, while in mild acid environment (pH 5.5), drug could be burst released

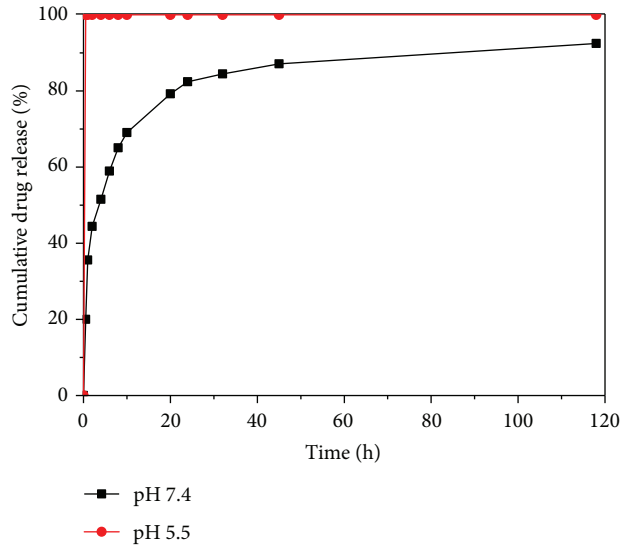

Figure 8: Cumulative CPT release behaviors in different medium pH values at 37°C.

from com-nano 1 within 30 min. The results indicated the pH-dependent drug-controlled release property for com-nano 1.

4. Conclusion

A magnetic and pH-sensitive composite nanoparticle could be easily fabricated by double water-in-oil-in-water (W/O/W) emulsion. The formed composite nanoparticle had similar surface chemical characteristic to pure Ac-β-CD nanoparticle; they exhibited both amorphous state of Ac-β-CD structure and some other crystal structure of Fe_3O_4 by XRD spectrum; they had three parts of obvious weight loss belonging to loss of bound water, degradation of acetal groups, and degradation of β-CD, respectively. Composite nanoparticle exhibited sphere and two-phase morphology with the diameter of about 200–250 nm depending on their detection method and zeta potential of −12 to −14 mV. The composite nanoparticle exhibited irreversible pH response property and reversible magnetic responsive properties either in neutral environment or in mild acid environment. Furthermore, the saturation magnetization of com-nano 1 and acid dissolved com-nano 1 was 0.2 and 0.8 emu/g. Finally, it was found that drug loading efficiency was 75%, and drug release behavior exhibited pH-dependent property through preliminary in vitro evaluation.

Conflicts of Interest

The authors declare that they have no conflicts of interest.

Acknowledgments

This study was financially supported by Natural Science Foundation of Jiangsu Province (BK20171113) and Qing Lan Project, six talent peaks project in Jiangsu Province (JY-071).

References

[1] Z. Chen, M. Sun, F. Luo, K. Xu, Z. Lin, and L. Zhang, "Stimulus-response click chemistry based aptamer-functionalized mesoporous silica nanoparticles for fluorescence detection of thrombin," *Talanta*, vol. 178, pp. 563–568, 2018.

[2] K. Kantak, Y. Black, E. Valencia, K. Green-Jordan, and H. Eichenbaum, "Stimulus-response functions of the lateral dorsal striatum and regulation of behavior studied in a cocaine maintenance/cue reinstatement model in rats," *Psychopharmacology*, vol. 161, no. 3, pp. 278–287, 2002.

[3] X. Zhang, J. Deng, Y. Xue, G. Shi, and T. Zhou, "Stimulus response of Au-NPs@GMP-Tb core-shell nanoparticles: toward colorimetric and fluorescent dual-mode sensing of alkaline phosphatase activity in algal blooms of a freshwater lake," *Environmental Science & Technology*, vol. 50, no. 2, pp. 847–855, 2015.

[4] S. Ast, P. J. Rutledge, and M. H. Todd, "pH-responsive quantum dots (RQDs) that combine a fluorescent nanoparticle with a pH-sensitive dye," *Physical Chemistry Chemical Physics*, vol. 16, no. 46, pp. 25255–25257, 2014.

[5] L. Ji, Z. Tan, T. R. Kuykendall et al., "Fe_3O_4 nanoparticle-integrated graphene sheets for high-performance half and full lithium ion cells," *Physical Chemistry Chemical Physics*, vol. 13, no. 15, pp. 7170–7177, 2011.

[6] P. Panneerselvam, N. Morad, and K. A. Tan, "Magnetic nanoparticle (Fe_3O_4) impregnated onto tea waste for the removal of nickel(II) from aqueous solution," *Journal of Hazardous Materials*, vol. 186, no. 1, pp. 160–168, 2011.

[7] B. Wang, P. Liu, B. Shi, J. Gao, and P. Gong, "Preparation of pH-sensitive dextran nanoparticle for doxorubicin delivery," *Journal of Nanoscience and Nanotechnology*, vol. 15, no. 4, pp. 2613–2618, 2015.

[8] L. Zhang, W. Hao, L. Xu et al., "A pH-sensitive methenamine mandelate-loaded nanoparticle induces DNA damage and apoptosis of cancer cells," *Acta Biomaterialia*, vol. 62, pp. 246–256, 2017.

[9] S. J. Lee, Y.-I. Jeong, H.-K. Park et al., "Enzyme-responsive doxorubicin release from dendrimer nanoparticles for anticancer drug delivery," *International Journal of Nanomedicine*, vol. 10, pp. 5489–5503, 2015.

[10] Y. Niu, F. J. Stadler, J. Song, S. Chen, and S. Chen, "Facile fabrication of polyurethane microcapsules carriers for tracing cellular internalization and intracellular pH-triggered drug release," *Colloids and Surfaces B: Biointerfaces*, vol. 153, pp. 160–167, 2017.

[11] N. Gooch, R. Burr, D. Holt, B. Gale, and B. Ambati, "Design and *in vitro* biocompatibility of a novel ocular drug delivery device," *Journal of Functional Biomaterials*, vol. 4, no. 1, pp. 14–26, 2013.

[12] S. Naahidi, M. Jafari, F. Edalat, K. Raymond, A. Khademhosseini, and P. Chen, "Biocompatibility of engineered nanoparticles for drug delivery," *Journal of Controlled Release*, vol. 166, no. 2, pp. 182–194, 2013.

[13] S. Rodrigues, M. Dionisio, C. R. Lopez, and A. Grenha, "Biocompatibility of chitosan carriers with application in drug delivery," *Journal of Functional Biomaterials*, vol. 3, no. 3, pp. 615–641, 2012.

[14] K. E. Broaders, J. A. Cohen, T. T. Beaudette, E. M. Bachelder, and J. M. J. Frechet, "Acetalated dextran is a chemically and biologically tunable material for particulate immunotherapy,"

Proceedings of the National Academy of Sciences of the United States of America, vol. 106, no. 14, pp. 5497–5502, 2009.

[15] X. Hu, S. Chen, X. Gong, Z. Gao, X. Wang, and P. Chen, "Synthesis and preparation of biocompatible and pH-responsive cyclodextrin-based nanoparticle," *Journal of Nanoparticle Research*, vol. 19, no. 3, p. 109, 2017.

[16] Z. Yu, R. Paul, C. Bhattacharya, T. C. Bozeman, M. J. Rishel, and S. M. Hecht, "Structural features facilitating tumor cell targeting and internalization by bleomycin and its disaccharide," *Biochemistry*, vol. 54, no. 19, pp. 3100–3109, 2015.

[17] Z. Yu, R. M. Schmaltz, T. C. Bozeman et al., "Selective tumor cell targeting by the disaccharide moiety of bleomycin," *Journal of the American Chemical Society*, vol. 135, no. 8, pp. 2883–2886, 2013.

[18] X. Hu, H. Tan, and L. Hao, "Functional hydrogel contact lens for drug delivery in the application of oculopathy therapy," *Journal of the Mechanical Behavior of Biomedical Materials*, vol. 64, pp. 43–52, 2016.

[19] X. Hu, H. Tan, X. Wang, and P. Chen, "Surface functionalization of hydrogel by thiol-yne click chemistry for drug delivery," *Colloids and Surfaces A: Physicochemical and Engineering Aspects*, vol. 489, pp. 297–304, 2016.

[20] X. Hu, D. Li, H. Tan, C. Pan, and X. Chen, "Injectable graphene oxide/graphene composite supramolecular hydrogel for delivery of anti-cancer drugs," *Journal of Macromolecular Science, Part A: Pure and Applied Chemistry*, vol. 51, no. 4, pp. 378–384, 2014.